INDIAN JOURNAL OF SCIENCE AND TECHNOLOGY

*Corresponding author.

gbsathishkumarmech@gmail.com

Surface modification of AZ61 Magnesium Alloy with Stelcar Alloy Powder Using Laser Cladding Technique

G B Sathishkumar[1]*, B Asaithambi[2], V Srinivasan[3]

1 Research Scholar, Department of Manufacturing Engineering, Faculty of Engineering and Technology, Annamalai University, Annamalai Nagar, Chidambaram, 608002, Tamil Nadu, India
2 Assistant Professor, Department of Manufacturing Engineering, Faculty of Engineering and Technology, Annamalai University, Annamalai Nagar, Chidambaram, 608002, Tamil Nadu, India
3 Associate Professor, Department of Manufacturing Engineering, Faculty of Engineering and Technology, Annamalai University, Annamalai Nagar, Chidambaram, 608002, Tamil Nadu, India

Abstract

Objective: To examine the tribological and mechanical characteristics of the AZ61 alloy reinforced with Stelcar alloy powder by surface modification through laser cladding. **Methods:** Surface modification was done by using a laser cladding machine, where the input parameters including Scanning Speed (SS), Laser Power (LP) and Powder Feed Rate (PFR) were adjusted. Experimental design followed a L9 Taguchi approach, and optimization of input parameters for the surface modified AZ61 alloy reinforced with Stelcar alloy particles was achieved using Grey Relational Analysis (GRA). Output responses, namely wear volume and micro hardness were measured to assess the effectiveness of the optimization process. **Findings:** From the results obtained through the experiments, powder feed rate contributes to 82.81% of the variability in wear volume, whereas the laser power mostly impacts micro hardness; influencing it by 89.46% confirmed with ANOVA. In order to determine the optimal processing parameters among various objectives, this research applies the grey relational method. The results showed that the wear volume and micro hardness of the composite were significantly affected by the Stelcar reinforcement. Employing Grey relational analysis combined with several optimization objectives into a transparent method, resulting in a clad material with the lower wear volume and higher micro hardness. The optimized processing parameters predicted grey relational grades with an error rate of 1.39% and a significant contribution of 63.60% from laser power. This study confirmed that multi-objective optimization could enhance laser-cladded surface mechanical characteristics and laid out the theoretical foundation for this approach. **Novelty:** This study introduces an innovative approach to surface modification by employing the laser cladding technique to reinforce Stelcar alloy particles, thereby creating a dense coating on the substrate.

1 Introduction

Since from the past few years of automotive industrial revolution, novel light-weight materials are in demand to satisfy the industrial need. AZ61 Magnesium alloys are promising structural materials widely used in automotive and aerospace industries because they are 35% lighter than aluminium alloys and 65 % lighter than titanium alloys[1]. Engine blocks, transmission casings, steering wheel frames, seat frames, and other automotive parts are increasingly made by using AZ61 magnesium alloys. However, Poor wear resistance, corrosion resistance and high temperature stability limit their industrial applications[2]. Laser cladding has emerged as a promising technique for modifying the surfaces of magnesium alloys, presenting numerous advantages compared to traditional coating methods like electroplating, thermal spraying, and physical vapor deposition. In contrast to conventional approaches that may encounter challenges such as inadequate adhesion, high porosity, and limited control over coating thickness, laser cladding offers precise control during the deposition process and enables the integration of reinforcing particles into the substrate[3]. Laser cladding (LC) is a newer surface modification process that utilizes a high-energy laser beam to melt and deposit coating material over the substrate, producing a coating deposition with superior metallic bonding and characteristics. The potential advantages of the coating deposited by laser cladding on the substrate include a low dilution rate, a small heat-affected zone, and excellent mechanical and physical qualities[4]. LC is a complex process involving laser, powder, substrate, and processing parameter setup interactions. The choice of processing parameters considerably impacts the formation and quality of coating deposition. Furthermore, the choice of process parameters differs depending on specific requirements. Multiple objectives are typically considered in real industrial applications, and an optimal process parameter setup is essential[5]. Several researchers have recently investigated the formation process and coating quality of laser cladding, and their findings are summarized below.

Lu et al. optimises laser cladding parameters for Ni60 coating on Q235 substrate. The study adjusts laser cladding parameters to improve Ni60 coating performance. The study examines how laser power, scanning speed, and powder feed rate affect coating microstructure and properties. The findings optimise the laser cladding process to improve Ni60 coating on friction and wear resistance for engineering applications[6]. In another study, Kumar et al. examines process parameters and characterization for laser cladding cBN-based composite over Ti6Al4V alloy. The study optimises laser cladding process parameters to improve composite clad coating properties and performance. Microstructure and wear resistance are assessed when characterizing the clad. The research helps to understand laser cladding and improve composite materials for engineering applications[7]. Xi et al. reported an analytical and predictive investigation of the geometric characteristics of multi-layer cladding layers of YCF102. The study seeks to understand and predict laser cladding layer geometry. Track offset, track overlap, and layer thickness are analysed to optimise laser cladding for geometric characteristics[8]. Ma et al. modeled and optimised laser cladding using multi-objective quantum-behaved particle swarm optimisation. The study seeks optimal processing parameters to improve composite material laser cladding coating properties and efficiency. The multi-objective quantum-behaved particle swarm optimisation algorithm found to be the best solution and improved laser cladding[9]. Fan et al. reported the laser-clad 15MnNi4Mo steel with Co-based powder containing 40% WC. They created a single-factor experiment to determine how processing parameters affected cladding layer geometric dimensions, dilution rate and hardness. They found

the best processing parameters based on coating hardness and dilution rate indices using an orthogonal experimental design. Finally, they created regression-based mathematical models [10].

Stelcar alloy powder (mixture of carbide particles and nickel or cobalt based powders) is commonly utilized as a reinforcing material in laser cladding due to its high hardness, wear resistance, good corrosion resistance and high-temperature strength as reported in previous research works. In the additive manufacturing industry, ensuring production efficiency is crucial for industrial applications [11]. This research aims at to investigate the influence of selected processing parameters on the properties of stelcar alloy powder coating using grey relational analysis and orthogonal experimental design. The current research on laser cladding has primarily focused on the geometric characteristics of the cladding layer, while investigations into the influence of processing parameters on multiple objectives simultaneously have been rare. In particular, there is a shortage of multiple-objective optimization methods that combine wear volume with micro hardness.

Based on the literature available the laser cladding represents a viable technique for surface modification, resulting in improved mechanical, wear, and corrosion properties. However, there is limited research on the utilization of Stelcar alloy powder for laser cladding of magnesium alloys. Additionally, no published reports are available regarding the optimization of hardness and wear resistance of AZ61 magnesium alloy through laser cladding with Stelcar alloy powder. Hence, this study aims at to examine the influence of different processing parameters, including laser power, scanning speed, and powder feed rate, on the surface modification of magnesium alloy substrates. The findings of this study provide a theoretical basis for multiple-objective optimization and predicting lower wear volume and higher micro hardness by adjusting processing parameters in laser cladding.

2 Methodology

2.1 Materials

The AZ61 magnesium alloy used in this study contained magnesium (Mg) – 92%, aluminum (Al) – 5.80 to 7.20%, zinc (Zn) – 0.40 to 1.50%, Manganese (Mn) - 0.15%, Silicon (Si) - 0.10%, Copper (Cu) - 0.050%, Nickel (Ni) - 0.0050%, and Iron (Fe) - 0.0050% and sourced as plates from Vision Castings and Alloys (Hyderabad), the alloy underwent pre-treatments before laser cladding to ensure a clean and uniform substrate, removing contaminants and oxides. A light polishing step followed to achieve a smooth surface, facilitating optimal adhesion of the cladding layer. Initial surface conditions were assessed through surface roughness measurements, providing crucial baseline data for evaluating the impact of laser cladding on surface modifications. To prevent contamination and oxidation during handling, AZ61 magnesium alloy specimens were stored in a controlled, low-humidity environment. The microstructure and elemental composition of the AZ61 magnesium alloy were analyzed using scanning electron microscopy (SEM) and energy dispersive X-ray spectroscopy (EDAX), as depicted in Figure 1 **(a & b)**. [12]

The Stelcar alloy powder used in this research was sourced from Zhangzhou Xiangcheng Yuteng Ceramic Products Co., Ltd (China), comprises Tungsten (W) - 48.3%, Nickel (Ni) - 33.3%, Carbon (C) - 11.8%, Iron (Fe) - 5.0%, Silicon (Si) - 1.0%, and Boron (B) - 0.6%, with a particle size distribution range of 50 – 120 microns. To address agglomerations or irregularities, a 10-minute controlled milling process at 400 rpm using a planetary ball-mill was employed. A specialized powder feeder, ensuring consistent and controlled powder flow, was used during laser cladding. Before laser cladding, the Stelcar alloy powder's characteristics, including morphology and chemical composition, were verified using SEM and EDAX as shown in Figure 1**(c & d)**. This verification ensured the quality and consistency of the powder for effective surface modification [13].

2.2 Experimental details

The laser cladding system, illustrated in Figure 2, was equipped with critical control parameters, including laser generation, powder feeding system, deposition system, and a PLC computer system. Prior to initiating the laser cladding process, meticulous preparation of the substrate surface was undertaken, encompassing thorough cleaning with acetone, rinsing with alcohol, and careful drying. Prior to treatment, images were captured to document the initial state of the substrate surface in Figure 3 **(a)**. The laser cladding process is intricate and subject to various influencing factors. This research investigates the effects of three crucial variables scanning speed, Laser power, and Powder feed rate with each set at three different levels. Employing a three-factor and three-level orthogonal array design, as detailed in Table 1, allowed for the exploration of these factors and their interactions with a minimized number of experimental runs, aiming for optimal results. Consequently, the L9 (3^3) Taguchi orthogonal array comprised a total of 9 trials, as elaborated in Table 1. After the laser cladding process, images were captured again to illustrate the surface modifications achieved in Figure 3 **(b)**. The thermal energy from the laser melts the Stelcar powder and the magnesium substrate, leading to alloying and mixing at the interface. This can result in the formation of a composite layer with improved hardness, wear resistance, and corrosion resistance compared to the untreated magnesium surface. Further, viable
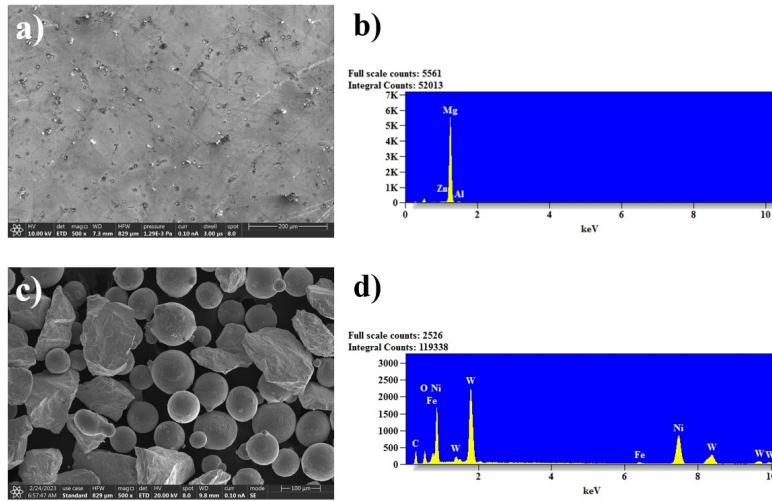
Fig 1. (a) SEM image of AZ61 Mg alloy (b) EDAX of AZ61 Mg alloy (c) SEM image of Stelcar powder (d) EDAX of Stelcar powder

pores and voids in the uncoated substrate has been filled and repaired post cladding. Upon completion of the laser cladding processes, the nine surface-modified samples were subjected to analysis to evaluate the wear volume and micro hardness of the clad properties[14].
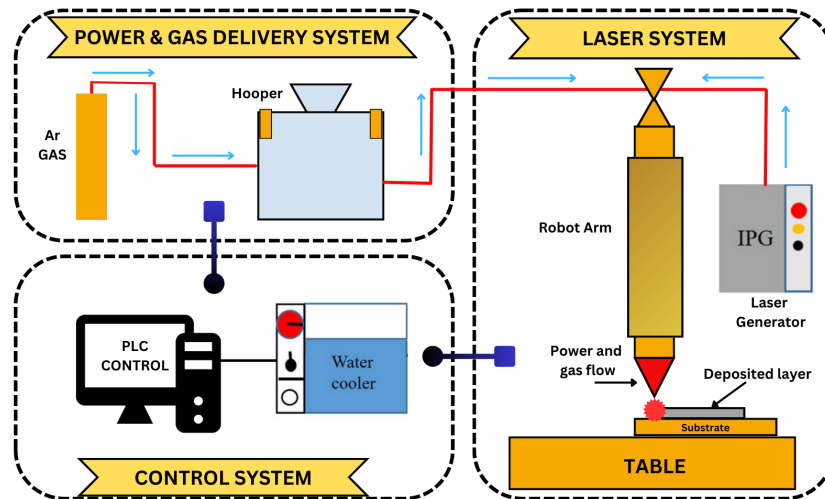
Fig 2. Schematic illustration of Laser Cladding System
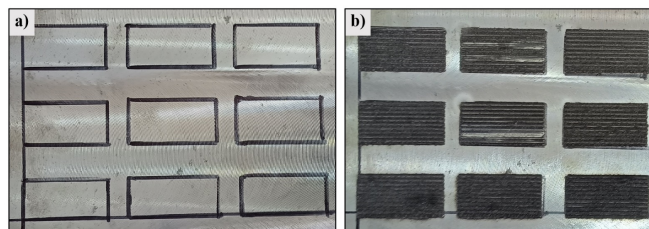
Fig 3. (a) Uncoated AZ61 Mg Alloy (b) Coated AZ61 Mg Alloy

The examination of micro hardness was carried out through a Vickers hardness tester, adhering to the ASTM E92 Standard, by analyzing the cross-section of the specimens. Specifically, the micro hardness of the AZ61 substrate subjected to laser cladding was evaluated under a load of 300 grams and a dwell time of 12 seconds. Throughout the testing process, hardness measurements were taken at 0.1 mm intervals from the surface to the interior of the treated AZ61 Mg alloy substrate, and subsequently, the average value was computed. This procedure and the setup of the Micro hardness testing machine are illustrated in Figure 4(a & b), respectively [15].
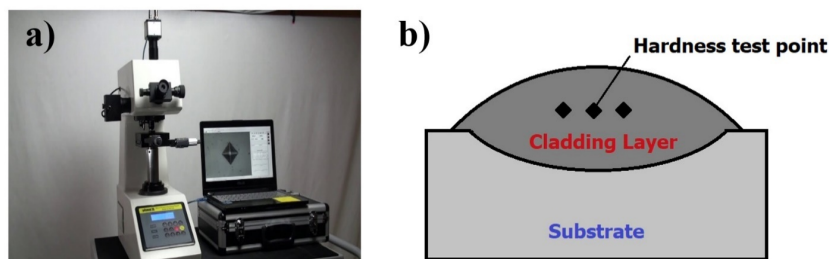
Fig 4. (a) Vickers Micro hardness Tester (b) Test Location of the Vickers indentation

The wear characteristics were assessed and studied using a pin-on-disc apparatus, as depicted in Figure 5. The dry sliding wear properties of the clad specimens were analyzed following ASTM G99 standards. Before conducting the wear behavior test, specimens were precisely cut using Wire Electrical Discharge Machining (WEDM) to dimensions of 10 mm in diameter and 30 mm in height from the modified surface specimens. These specimens were then tested against a counter surface of EN 32 steel disc with a hardness rating of 60 HRC. Both surfaces underwent cleaning with acetone solvent before the wear test. To investigate the wear behavior of laser-clad samples, an applied load of 20 N, a sliding speed of 1.25 m/s, and a sliding distance of 800 m were utilized. The surface morphologies of the wear-tested clad specimens were examined using SEM to identify wear scars and mechanisms [16].
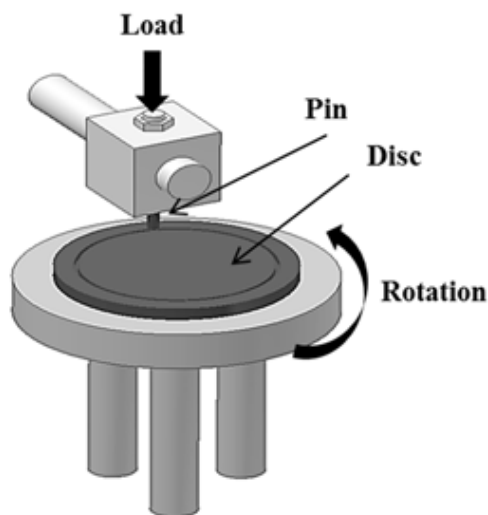
Fig 5. Schematic illustration of Pin on disc apparatus

3 Results and discussion

Laser cladding was employed with Stelcar powder to alter AZ61, following the Taguchi experimental approach for designing the plan, which encompassed factors like scanning velocity, laser power, and powder feed rate. The study investigated wear characteristics and micro hardness of the surface-treated AZ61 magnesium alloy, with data recorded under room temperature conditions. Table 1 illustrates the utilization of Taguchi's Design of Experiments (DoE) methodology in crafting an experiment

for surface modification, utilizing specified variables and their respective levels.

Table 1. Expanded L9 of process parameters and output responses

Trial No	Scanning speed (mm/s)	Laser power (kW)	Powder feed rate (g/m)	Wear volume (mm^3)	Microhardness (HV)
1	8	1.2	30	1.5417	582.05
2	8	1.3	35	1.0981	664.85
3	8	1.4	40	1.1841	613.68
4	9	1.2	35	1.1721	570.78
5	9	1.3	40	1.2138	675.83
6	9	1.4	30	1.4053	619.81
7	10	1.2	40	1.2155	615.51
8	10	1.3	30	1.3501	669.81
9	10	1.4	35	0.9782	622.10

The research utilized the signal-to-noise (S/N) ratio method in conjunction with Taguchi analysis to determine the optimal processing parameters for the laser cladding procedure. This S/N conversion serves as a critical tool for refining data analysis and improving tribological and mechanical properties to achieve ideal outcomes. Key factors such as micro hardness and wear volume of the laser-cladded surface were of utmost significance, with the preference for 'lesser is better' for wear volume and 'larger is better' for micro hardness. The S/N ratio for these attributes was computed using real data extracted from Table 1. The results of the S/N conversion, alongside measured values for wear volume and micro hardness, are presented in Table 2. Subsequently, Analysis of Variance (ANOVA) was applied to investigate the factors influencing wear volume and micro hardness with a 95% confidence interval, supported by Design of Experiments.

Table 2. Results of S/N conversion for Wear volume and Micro hardness

Trial No.	Wear volume	S/N of wear volume	Micro hardness	S/N of Micro hardness
1	1.5417	-3.76000	582.05	55.2992
2	1.0981	-0.81284	664.85	56.4545
3	1.1841	-1.46777	613.68	55.7588
4	1.1721	-1.37929	570.78	55.1294
5	1.2138	-1.68294	675.83	56.5967
6	1.4053	-2.95538	619.81	55.8452
7	1.2155	-1.69510	615.51	55.7847
8	1.3501	-2.60732	669.81	56.5190
9	0.9782	0.19145	622.10	55.8772

3.1 ANOVA Variance Analysis

The ANOVA method was utilized to assess the optimal data by utilizing the S/N ratio table. Prior to employing ANOVA, the Anderson–Darling (AD) test was conducted to verify normality. A p-value exceeding 0.05 indicates a normal distribution. The p-values obtained from the AD test, after transforming S/N values of micro hardness and wear volume, were indeed greater than 0.05, as depicted in Figure 6**(a & b)**. With the confirmation of normal distribution in the responses, ANOVA analysis was carried out accordingly[17].

3.2 Influence of Control Variables on Wear Volume

The wear volume analysis presented in Table 3 revealed the contribution percentages of the factors as follows: powder feed rate accounted for 82.81%, laser power for 10.28%, scanning speed for 6.85%, and error for 0.05%. These findings highlight that the powder feed rate had the most notable influence on wear volume, largely attributed to the utilization of Stelcar alloy powder.

Figure 7 illustrates the average Signal-to-Noise ratio of wear volume across different factors and their levels, indicating that powder feed rate exerts the greatest influence. According to Figure 7, derived from the S/N ratio response table, the third level of scanning speed, laser power and second level of powder feed rate appears to be optimal for achieving high S/N ratios and
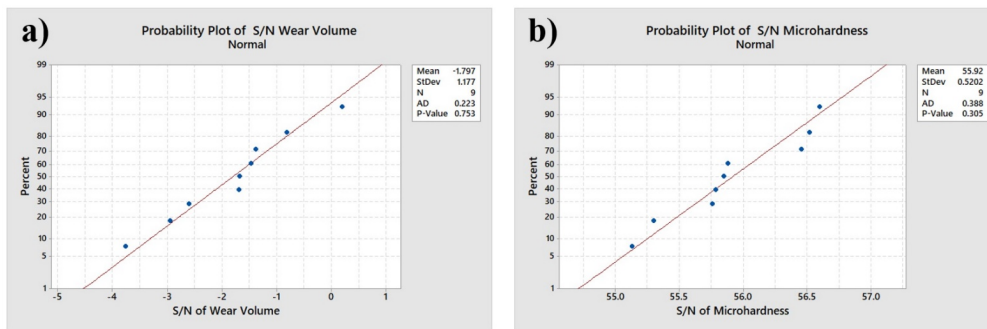
Fig 6. (a) Normality test for S/N of Wear volume and (b) Normality test for S/N of Micro hardness

Table 3. S/N of Wear volume ANOVA analysis

Source	DF	Seq SS	Contribution	Adj SS	Adj MS	F-Value	P-Value
SS (mm/s)	2	0.015637	6.85%	0.015637	0.007818	124.70	0.008
LP (kW)	2	0.023465	10.28%	0.023465	0.011733	187.13	0.005
PFR (g/m)	2	0.188938	82.81%	0.188938	0.094469	1506.74	0.001
Error	2	0.000125	0.05%	0.000125	0.000063		
Total	8	0.228166	100.00%				

minimizing wear volume. An elevation in powder feed rate notably decreases wear loss, likely due to constraints on the plastic deformation of the AZ61 Mg alloy induced by the presence of Stelcar. Consequently, this enhances the hardness of the cladded structure, leading to reduced wear loss. These observations align with the findings reported by Guofu Lian et al. [18].
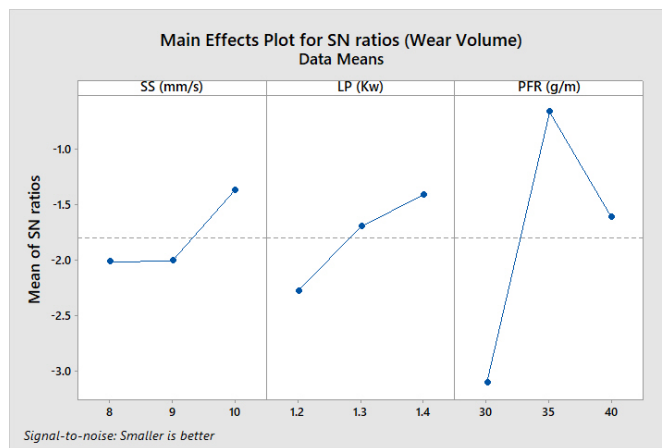
Fig 7. S/N of Wear volume with main effects plot

3.3 Influence of Control Variables on Micro hardness

Table 4 exhibits the ANOVA findings concerning the signal-to-noise ratio of micro hardness. The p-value associated with laser power was 0.034, which was notably less than the 0.05 significance threshold, suggesting a noteworthy impact of laser power on micro hardness. Laser power accounted for 89.46% of the variability observed in micro hardness, rendering it the primary influencing factor, trailed by scanning speed at 3.88% and powder feed rate at 3.51%.

The results depicted in Figure 8 display the averaged signal-to-noise ratio of micro hardness across different levels of each factor. Among these factors, laser power emerged as the most influential, as indicated by the delta value, representing the maximum of means. The main effect plot depicted in Figure 8 illustrates that increasing laser power significantly enhances

Table 4. S/N of Micro hardness ANOVA analysis

Source	DF	Seq SS	Contribution	Adj SS	Adj MS	F-Value	P-Value
SS (mm/s)	2	434.3	3.88%	434.3	217.2	1.23	0.448
LP (kW)	2	10027.0	89.46%	10027.0	5013.5	28.42	0.034
PFR (g/m)	2	393.7	3.51%	393.7	196.8	1.12	0.473
Error	2	352.8	3.15%	352.8	176.4		
Total	8	11207.8	100.00%				

micro hardness. Optimal values were attained at the third level of scanning speed, second level of laser power, and third level of powder feed rate, as indicated by the S/N ratio effect plot. These optimal parameters were determined to be 10 mm/s of scanning speed, 1.3 kW of laser power and 40 g/m of powder feed rate. This observation aligns with findings reported by Guofu Lian et al. in their research[18].
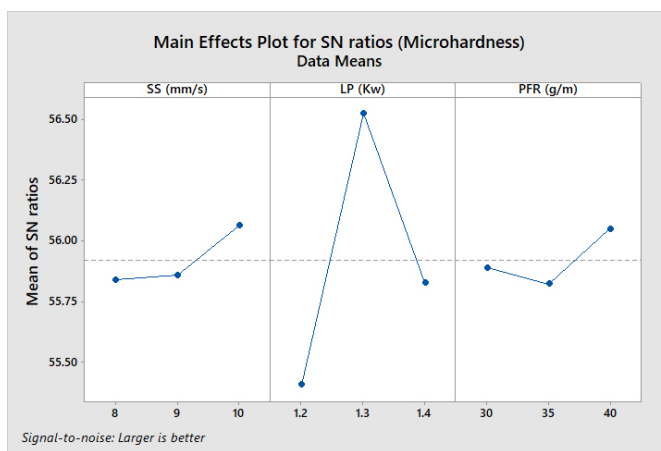
Fig 8. S/N of Micro hardness with main effects plot

3.4 Grey Relational Analysis of Mechanical Responses

This study introduces an optimization approach that combines grey relational analysis with the Taguchi (DoE) technique. The objective is to simultaneously reduce wear volume and enhance micro hardness. While Taguchi orthogonal experiment design and ANOVA are effective for single-objective optimization, they have limitations in multi-objective scenarios. Grey relational analysis is employed here to identify the optimal processing settings considering both wear volume and micro hardness responses. The normalization technique within GRA is suggested as an effective strategy for optimizing complex relationships among multiple performance parameters. GRA assesses various performance characteristics within a Grey Relational Grade (GRG).

The steps involved in GRA data processing are outlined as follows:

Step 1: S/N Ratio Normalization and Deviation:

The initial step in GRA entails normalizing and deviating the experimental data to fall within the range of 0-1. In this analysis, lower wear volume signifies superior performance ("lower-is-better"), while higher micro hardness corresponds to better cladding performance ("higher-is-better")[19]. The normalized wear volume and micro hardness values are computed using Equations (1) and (2) respectively. The deviation sequence values are presented in Table 5.

Smaller the better option:

$$Y_i(p) = \frac{maxX_i(p) - X_i(p)}{maxX_i(p) - minX_i(p)} \tag{1}$$

Larger the better option:

$$Y_i(p) = \frac{X_i(p) - minX_i(p)}{maxX_i(p) - minX_i(p)} \tag{2}$$

Step – 2: Grey Relation Coefficient (GRC) Calculation :

Following the normalization of the S/N ratio, the GRC is calculated by using the Equation (3).

$$GRC_i(p) = \frac{\Delta_{min}(p) + \delta\Delta_{max}(p)}{\Delta_i(p) + \delta\Delta_{max}(p)} \tag{3}$$

Step 3: Calculation of Grey Relational Grade (GRG):

The GRG is determined using Equation (4), which assigns equal importance to both micro hardness and wear volume responses.

$$GRC_i = \frac{1}{n}\sum_{p=1}^{n} GRC_i(p) \tag{4}$$

The tabulated figures in Table 5 display the computed normalization values, as well as the GRC and GRG for all experimental runs. Subsequently, an ANOVA was performed. Table 6 depicts the analysis outcomes concerning the input variables and their respective impacts on the overall grey relational grade: laser power accounted for 63.60%, powder feed rate for 24.90%, and scanning speed for 10.11%. Additionally, Table 5 provides the overall GRG ranking, highlighting the fifth run as optimal, characterized by scanning speed of 9 m/s, laser power of 1.3 kW, and powder feed rate of 40 g/m. Furthermore, Figure 9 illustrates the rank order for GRG alongside mechanical responses.

Table 5. Data normalization, deviation, GRC and GRG values

Trial No.	S/N of Wear volume			S/N of Micro hardness			GRG	Rank
	Normalized	Deviation	GRC	Normalized	Deviation	GRC		
1	0.0000	1.0000	0.3333	0.1073	0.8927	0.3590	0.3462	9
2	0.7872	0.2128	0.7015	0.8955	0.1045	0.8271	0.7643	2
3	0.6346	0.3654	0.5778	0.4084	0.5916	0.4580	0.5179	5
4	0.6559	0.3441	0.5923	0.0000	1.0000	0.3333	0.4628	7
5	0.5819	0.4181	0.5446	1.0000	0.0000	1.0000	0.7723	1
6	0.2421	0.7579	0.3975	0.4667	0.5333	0.4839	0.4407	8
7	0.5789	0.4211	0.5428	0.4258	0.5742	0.4655	0.5041	6
8	0.3400	0.6600	0.4310	0.9427	0.0573	0.8972	0.6641	4
9	1.0000	0.0000	1.0000	0.4885	0.5115	0.4943	0.7472	3

Table 6. S/N of grey relational grade ANOVA analysis

Source	DF	Seq SS	Contribution	Adj SS	Adj MS	F-Value	P-Value
SS (mm/s)	2	4.9931	10.11%	4.9931	2.4965	7.26	0.121
LP (kW)	2	31.4043	63.60%	31.4043	15.7021	45.64	0.021
PFR (g/m)	2	12.2931	24.90%	12.2931	6.1465	17.87	0.053
Error	2	0.6880	1.39%	0.6880	0.3440		
Total	8	49.3784	100.00%				

3.5 Experimental Validation

The last stage entails experimental validation and evaluation of performance characteristics. After acquiring the best input parameter values, this validation experiment employs the same configuration with these values, measuring output responses. Table 7 displays both predicted and observed response values alongside their respective percentage errors during the experimental validation of the developed model. The highest error recorded is 1.04%, suggesting a strong correlation between predicted and observed values.

3.6 Wear Mechanism

Analysis of wear mechanisms indicated that increasing the powder feed rate resulted in a decrease in wear volume and enhanced wear resistance by restricting plastic deformation and bolstering protection of the AZ61 matrix. Figure 10**(a)** illustrates that
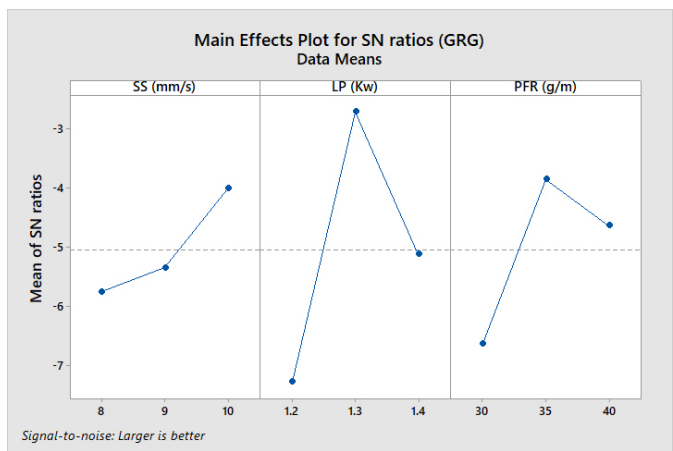
Fig 9. S/N of GRG with main effects plot

Table 7. Experimental validation and comparison

Input parameters / Output r esponses	5ᵗʰ run [Taguchi design]	Predicted optimal set	Experimental validation
Scanning Speed (mm/s)	9	10	10
Laser Power (kW)	1.3	1.3	1.3
Powder Feed Rate (g/m)	40	35	35
Wear volume (mm^3)	1.2138	-	1.0985
Micro hardness (HV)	675.83	-	670.12
GRG	0.7723	0.8118	0.8014

elevating the powder feed rate is associated with thicker coatings, leading to a decrease in the wear rate. Notably, the presence and impact of Stelcar particles on worn surfaces are clearly evident, showing minimal plastic deformation of the Mg matrix and grooved lines from interaction with the hard counter surface. With higher powder feed rates of Stelcar particles, plastic drift, crater formation, and ploughing marks are notably reduced, suggesting that composite coatings with increased Stelcar particles offer improved protection to the underlying softer Mg-based alloy, resulting in reduced wear and fewer deep plough grooves. However, Figure 10 **(b)** reveals a different aspect of the wear mechanism, indicating the formation of a tribo layer when the powder feed rate exceeds 35 g/min. While generally beneficial, the effectiveness of this layer is constrained by the aggregation of Stelcar particles within the matrix phase. The presence of isolated patches of the tribo layer on the worn surface suggests an optimal concentration of Stelcar particles for achieving optimal tribological performance [20].
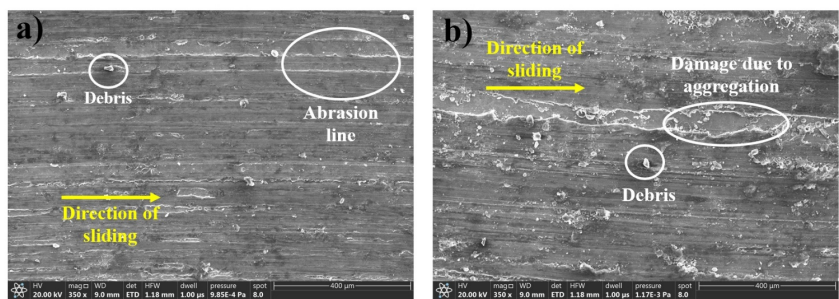
Fig 10. SEM analysis on worn surfaces a) Low Wear Loss b) High Wear Loss

4 Conclusion

This study employs Taguchi orthogonal design to evaluate how processing parameters (specifically scanning speed, laser power, and powder feed rate) affect the wear volume and micro hardness of laser-cladded AZ61 Mg alloy. Both signal-to-noise ratio conversion and multi-objective grey relational analysis were employed to optimize achieving minimum wear volume (1.0985 mm^3) and maximum hardness (670.12 HV). Experimental validation of these processing parameters confirmed the effectiveness of this method. The primary findings derived from this investigation are summarized as follows:

1. In the analysis of micro hardness, the main sequence of processing parameters observed was LP, SS, and PFR. Laser power was found to have a notable impact on micro hardness, enhancing it as the laser power was increased up to 1.3 kW. However, beyond this threshold, hardness levels decreased due to the formation of a larger melt pool on the substrate surface.

2. Analysis of volume wear revealed that the sequence of parameters was PFR, LP, and SS. The powder feed rate demonstrated a notable impact on wear volume, with a decrease observed in wear volume with the powder feed rate rising up to 35 g/min. However, beyond this threshold, wear volume increased due to heightened inclusion of particles. Inadequate melting and bonding among particles, alongside the formation of undesirable phases or microstructures, weakened the clad layer, leading to reduced hardness and ultimately diminished wear resistance.

3. In the context of evaluating wear volume and hardness through grey relational analysis, the ordered processing parameters are as follows: laser power accounts for 63.60%, powder feed rate for 24.90%, and scanning speed for 10.11%. Notably, both laser power and powder feed rate demonstrate statistical significance in this analysis.

4. The lowest wear volume and highest micro hardness were achieved with the ideal processing conditions of 10 mm/s scanning speed, a laser power of 1.3 kW, and a powder feed rate of 35 g/min.

Future scope of work

To explore the mechanical, tribological, and corrosion characteristics of AZ61 enhanced with Stelcar alloy powder through surface modification via laser cladding, the study aims at to optimize process parameters such as scanning speed, laser power, powder feed rate, and gas flow rate using a Taguchi experimental design (L16) for future investigations.

References

1) Liu B, Yang J, Zhang X, Yang Q, Zhang J, Li X. Development and application of magnesium alloy parts for automotive OEMs: A review. *Journal of Magnesium and Alloys*. 2023;11(1):15–47. Available from: https://dx.doi.org/10.1016/j.jma.2022.12.015. doi:10.1016/j.jma.2022.12.015.

2) Prasad SVS, Prasad SB, Verma K, Mishra RK, Kumar V, Singh S. The role and significance of Magnesium in modern day research-A review. *Journal of Magnesium and Alloys*. 2022;10(1):1–61. Available from: https://dx.doi.org/10.1016/j.jma.2021.05.012. doi:10.1016/j.jma.2021.05.012.

3) Yang D, editor. Practical Applications of Laser Ablation. IntechOpen. 2021. Available from: https://doi.org/10.5772/intechopen.94439. doi:10.5772/intechopen.92496.

4) Zhao P, Shi Z, Wang X, Li Y, Cao Z, Zhao M, et al. A Review of the Laser Cladding of Metal-Based Alloys, Ceramic-Reinforced Composites, Amorphous Alloys, and High-Entropy Alloys on Aluminum Alloys. *Lubricants*. 2023;11(11):1–29. Available from: https://dx.doi.org/10.3390/lubricants11110482. doi:10.3390/lubricants11110482.

5) Zhu L, Xue P, Lan Q, Meng G, Ren Y, Yang Z, et al. Recent research and development status of laser cladding: A review. *Optics & Laser Technology*. 2021;138:106915. Available from: https://dx.doi.org/10.1016/j.optlastec.2021.106915. doi:10.1016/j.optlastec.2021.106915.

6) zheng Lu P, Jia L, Zhang C, Heng X, chen Xi X, fan Duan M, et al. Optimization on laser cladding parameters for preparing Ni60 coating along with its friction and wear properties. *Materials Today Communications*. 2023;37:107162. Available from: https://dx.doi.org/10.1016/j.mtcomm.2023.107162. doi:10.1016/j.mtcomm.2023.107162.

7) Kumar S, Mandal A, Das AK. The effect of process parameters and characterization for the laser cladding of cBN based composite clad over the Ti6Al4V alloy. *Materials Chemistry and Physics*. 2022;288:126410. Available from: https://dx.doi.org/10.1016/j.matchemphys.2022.126410. doi:10.1016/j.matchemphys.2022.126410.

8) Xi W, Song B, Chen L, Liang Y, Yu T, Wang J, et al. Multi-track, multi-layer cladding layers of YCF102: An analytical and predictive investigation of geometric characteristics. *Optics & Laser Technology*. 2023;167:109696. Available from: https://dx.doi.org/10.1016/j.optlastec.2023.109696. doi:10.1016/j.optlastec.2023.109696.

9) Ma M, Xiong W, Lian Y, Han D, Zhao C, Zhang J. Modeling and optimization for laser cladding via multi-objective quantum-behaved particle swarm optimization algorithm. *Surface and Coatings Technology*. 2020;381:125129. Available from: https://dx.doi.org/10.1016/j.surfcoat.2019.125129. doi:10.1016/j.surfcoat.2019.125129.

10) Bourahima F, Helbert AL, Ji V, Rege M, Courteaux A, Brisset F, et al. Optimization of Microstructural Evolution during Laser Cladding of Ni Based Powder on GCI Glass Molds. *Key Engineering Materials*. 2019;813:185–190. Available from: https://dx.doi.org/10.4028/www.scientific.net/kem.813.185. doi:10.4028/www.scientific.net/kem.813.185.

11) Bartkowski D, Bartkowska A, Olszewska J, Przestacki D, Ulbrich D. Stellite-6/(WC+TiC) Composite Coatings Produced by Laser Alloying on S355 Steel. *Materials*. 2023;16(14):1–19. Available from: https://dx.doi.org/10.3390/ma16145000. doi:10.3390/ma16145000.

12) Sathish T, Mohanavel V, Ansari K, Saravanan R, Karthick A, Afzal A, et al. Synthesis and Characterization of Mechanical Properties and Wire Cut EDM Process Parameters Analysis in AZ61 Magnesium Alloy + B4C + SiC. *Materials*. 2021;14(13):1–21. Available from: https://dx.doi.org/10.3390/ma14133689. doi:10.3390/ma14133689.

13) Zhu ZY, Ouyang C, Chen JH, Qiao YX. Microstructure and mechanical properties of Stellite 6 alloy powders incorporated with Ti/B4C using plasma-arc-surfacing processes. *Materiali in tehnologije / Materials and technology*. 2019;53(1):3–8. Available from: https://dx.doi.org/10.17222/mit.2018.044. doi:10.17222/mit.2018.044.

14) Wang K, Liu W, Hong Y, Sohan H, Tong Y, Hu Y, et al. An Overview of Technological Parameter Optimization in the Case of Laser Cladding. *Coatings*. 2023;13(3):1–26. Available from: https://dx.doi.org/10.3390/coatings13030496. doi:10.3390/coatings13030496.

15) Devaraj LD, Srinivasan V. Evaluation of Micro Hardness and Wear Characteristics of Gyroid Designed Ti-6Al-4V Fabricated Through DMLS Technique. *Indian Journal Of Science And Technology*. 2023;16(47):4469–4480. Available from: https://doi.org/10.17485/IJST/v16i47.2637. doi:10.17485/IJST/v16i47.2637.

16) Mohankumar A, Duraisamy T, Packkirisamy V, Sampathkumar D. Response Surface Methodology and Mayfly Optimization for Predicting the Properties of Cold-Sprayed AA2024/Al2O3 Coatings on AZ31B Magnesium Alloy. *Journal of Materials Engineering and Performance*. 2023;p. 1–19. Available from: https://dx.doi.org/10.1007/s11665-023-08898-y. doi:10.1007/s11665-023-08898-y.

17) Ashokkumar M, Thirumalaikumarasamy D, Sonar T, Vignesh P, Deepak S. Optimization of cold spray coating parameters using RSM for reducing the porosity level of AA2024/Al2O3 coating on AZ31B magnesium alloy. *International Journal on Interactive Design and Manufacturing (IJIDeM)*. 2023;p. 1–15. Available from: https://doi.org/10.1007/s12008-023-01597-x. doi:10.1007/s12008-023-01597-x.

18) Lian G, Xiao S, Zhang Y, Jiang J, Zhan Y. Multi-objective optimization of coating properties and cladding efficiency in 316L/WC composite laser cladding based on grey relational analysis. *The International Journal of Advanced Manufacturing Technology*. 2021;112(5-6):1449–1459. Available from: https://dx.doi.org/10.1007/s00170-020-06486-1. doi:10.1007/s00170-020-06486-1.

19) Mugilan T, Sridhar N, Sathishkumar GB. Multi response hybrid optimization of sustainable high-speed end milling on 89.7Ti-6Al-4V. *Materials Today: Proceedings*. 2022;65(Part B):3170–3176. Available from: https://dx.doi.org/10.1016/j.matpr.2022.05.362. doi:10.1016/j.matpr.2022.05.362.

20) Sathishkumar GB, Asaithambi B, Srinivasan V. Optimizing Laser Cladding Parameters on AZ61 Magnesium Alloy with Inconel 625 Powder through Grey Relation Analysis. *Indian Journal of Science and Technology*. 2024;17(11):1059–1069. Available from: https://doi.org/10.17485/IJST/v17i11.2686. doi:10.17485/IJST/v17i11.2686.